

High Throughput Probabilistic Shaping with Product Distribution Matching

Georg Böcherer, *Member, IEEE*, Fabian Steiner, *Student Member, IEEE*, Patrick Schulte, *Student Member, IEEE*

Abstract—Product distribution matching (PDM) is proposed to generate target distributions over large alphabets by combining the output of several parallel distribution matchers (DMs) with smaller output alphabets. The parallel architecture of PDM enables low-complexity and high-throughput implementation. PDM is used as a shaping device for probabilistic amplitude shaping (PAS). For 64-ASK and a spectral efficiency of 4.5 bits per channel use (bpcu), PDM is as power efficient as a single full-fledged DM. It is shown how PDM enables PAS for parallel channels present in multi-carrier systems like digital subscriber line (DSL) and orthogonal frequency-division multiplexing (OFDM). The key feature is that PDM shares the DMs for lower bit-levels among different sub-carriers, which improves the power efficiency significantly. A representative parallel channel example shows that PAS with PDM is 0.93 dB more power efficient than conventional uniform signaling and PDM is 0.35 dB more power efficient than individual per channel DMs.

Index Terms—Probabilistic amplitude shaping, Distribution matcher, Rate adaptation, Parallel channels, Bit Loading, DSL, OFDM, Coded modulation

I. INTRODUCTION

Higher-order modulation is indispensable in mobile, satellite, cable, and fiber-optic communication to achieve the high spectral efficiency (SE) required for data applications.

Transceivers must be flexible, i.e., they should support different SEs so they can adapt to the link quality at hand and deliver the best possible connectivity. Conventional coded modulation uses uniform distributions on the constellation points. This has two disadvantages. First, uniform distributions suffer a power inefficiency of up to 1.53 dB. Second, flexibility can be achieved only by supporting a large number of modcods, i.e., combinations of modulation formats and channel codes. For example DVB-S2X requires supporting 116 modcods [1].

One approach that has been proposed is geometric shaping (GS) [2], [3] which uses constellations with non-equidistant signal points. While improved power efficiency was observed, the problem of flexibility remains. A second approach is probabilistic shaping (PS) that uses equidistant signal points with a non-uniform distribution. For an overview of PS schemes, see [4, Sec. II] and references therein. Recently, we proposed probabilistic amplitude shaping (PAS) [4], a PS architecture that concatenates a distribution matcher (DM) [5],

G. Böcherer, F. Steiner, P. Schulte are with the Institute for Communications Engineering, Technical University of Munich (TUM).

The work was partly supported by the German Federal Ministry of Education and Research in the framework of an Alexander von Humboldt Professorship.

The ideas presented in this work have been filed as a patent application with the EPO (application number: EP16192404.8) on October 5, 2016.

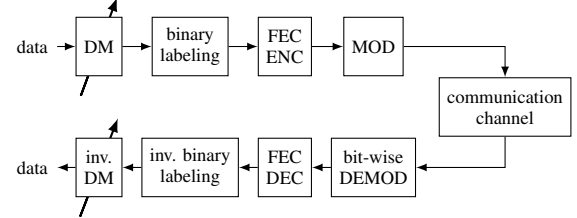


Fig. 1. System model of PAS. The shaping device DM is concatenated in reverse with the FEC device.

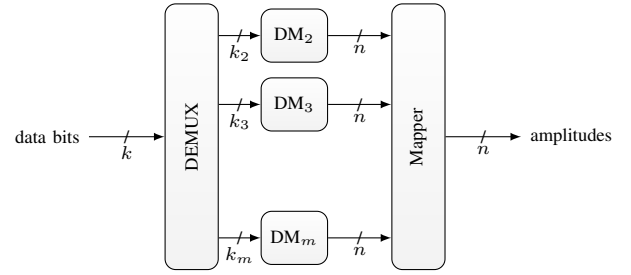


Fig. 2. The DM implementation proposed in this work: Product Distribution Matching (PDM) for 2^m -ASK. k binary data bits are demultiplexed into $m-1$ parallel blocks of sizes k_2 to k_m . Parallel binary component DMs output m shaped sequences of length n . A bit-mapper recombines the $m-1$ sequences and outputs one shaped amplitude sequence of length n .

[6] as a shaping device with forward error correction (FEC), see Fig. 1. PAS achieves the optimal power efficiency and enables flexible SE with only one FEC code [4, Sec. VIII]. PAS has been successfully integrated with low-density parity-check (LDPC) codes [4], turbo codes [7], SC-LDPC codes [8], polar codes [9], and nonbinary codes [10]. In comparison [11], PAS is over 0.3 dB more power efficient than Non-Uniform Constellations (NUC) [3], a GS implementation advocated by the Advanced Television Systems Committee (ATSC) 3.0 standard [12]. The benefits of PAS for fiber-optic communication were recently showcased in a field trial [13] and future optical modems will implement PS [14, Sec. V-A].

The enabling technology for PAS is the DM, which transforms a binary data sequence into a sequence of symbols with a desired distribution. For an overview of existing DM algorithms, see [6, Sec. I] and references therein. For implementation, fixed-to-fixed length DMs are desirable. For high-throughput applications, efficient DM encoding is required. Furthermore, fixed-to-fixed length DMs require a large block length to work well [15].

In many practical settings, the data link is well modelled by a set of non-interacting parallel channels. Examples in-

clude multi-carrier transmission such as orthogonal frequency division multiplexing (OFDM), discrete multitone (DMT), and multi-antenna transceivers when the singular value decomposition (SVD) of the channel matrix is used to orthogonalize the system. Employing current DM algorithms in such scenarios is challenging, as techniques like bit-loading partition the transmitted sequence in several short segments, each with an individual constellation size and distribution, which potentially causes a significant rate loss.

In this work, we propose a novel DM architecture called product distribution matching (PDM), which internally uses a collection of parallel DMs with smaller output alphabets to synthesize the desired distribution as a product distribution. A preferable implementation uses binary output alphabets for the individual DMs. This approach both facilitates high-throughput applications by parallelization and reduces the rate loss for short output lengths, which makes the PDM particularly amenable for large constellations and high-throughput. In the final part of this work, we propose extended PDM for parallel channels, which shares the component DMs for lower bit-levels among different sub-carriers. Extended PDM can be applied, e.g., in OFDM and DMT. We provide a representative example where extended PDM is 0.93 dB and 0.35 dB more power efficient than uniform signaling and individual per sub-carrier DMs, respectively, and operates close to the waterfilling limit. All simulation results were obtained using the DM implementations by [16].

This work is structured as follows. Sec. II reviews DMs and PAS and states achievable rate expressions for system design. In Sec. III, we introduce the PDM architecture and present finite length simulation results for 64-QAM. Sec. IV shows how extended PDM can be used to operate PAS close to the waterfilling limit of parallel channels. We conclude in Sec. V.

II. PRELIMINARIES

A. Distribution Matching (DM)

DMs [5], [6] transform a sequence of uniformly distributed input bits into an output sequence of symbols from an alphabet \mathcal{A} with a desired distribution. A fixed-to-fixed length DM maps k input bits d^k to n output symbols $a^n = \text{dm}(d^k)$. The mapping dm is invertible, i.e., d^k can be recovered from a^n by applying the inverse mapping dm^{-1} . Fixed-to-fixed length DMs can be implemented by the constant composition distribution matcher (CCDM) [6], for binary output alphabets see also [17]. A DM is characterized by the following parameters.

- The rate is

$$R_{\text{dm}} = \frac{k}{n} \left[\frac{\text{bits}}{\text{output symbol}} \right]. \quad (1)$$

- The output distribution is

$$P_A(a) = \frac{\sum_{d^k \in \{0,1\}^k} P_{\text{dm}(d^k)}(a)}{2^k}, \quad a \in \mathcal{A} \quad (2)$$

where P_{a^n} is the empirical distribution of the sequence a^n , i.e.,

$$P_{a^n}(a) = \frac{|\{i: a_i = a\}|}{n}, \quad a \in \mathcal{A}. \quad (3)$$

TABLE I
TWO LABELS FOR 8-ASK. THE AMPLITUDE LABEL OF NBBC IS NBC
AND THE AMPLITUDE LABEL OF BRGC IS ALSO BRGC.

	-7	-5	-3	-1	1	3	5	7
BRGC	000	001	011	010	110	111	101	100
NBBC	000	001	010	011	111	110	101	100

- The rate loss is the difference of the DM rate and the entropy rate of a discrete memoryless source (DMS) P_A , i.e.,

$$R_{\text{loss}} = \mathbb{H}(A) - \frac{k}{n}. \quad (4)$$

By [6, Sec. III.B], the rate loss of CCDM vanishes for large output lengths n . In this work, we are interested in DMs with relatively short output lengths and we therefore need to account for the rate loss in our system design.

B. Amplitude Shift Keying Modulation

We consider 2^m -amplitude shift keying (ASK) constellations

$$\mathcal{X} = \{\pm 1, \pm 3, \dots, \pm(2^m - 1)\} \quad (5)$$

with amplitude alphabet

$$\mathcal{A} = \{1, 3, \dots, 2^m - 1\}. \quad (6)$$

We use label functions $\beta: \mathcal{X} \rightarrow \{0, 1\}^m$ and corresponding bit mappers $\chi: \{0, 1\}^m \rightarrow \mathcal{X}$. For all labels $\mathbf{B} = B_1 \dots B_m$ in this work, the first bit B_1 labels the sign S according to

$$B_1 = \begin{cases} 0, & S = 1 \\ 1, & S = -1. \end{cases} \quad (7)$$

Consequently, $B_2 \dots B_m$ label the amplitudes and each label function β implies an amplitude label function β_A and each bit-mapper χ implies an amplitude bit-mapper χ_A . Two labels are of special interest, namely the binary reflected Gray code (BRGC) [18] and the natural based binary code (NBBC) [4, Sec. VI.C] where the amplitude label is a natural binary code (NBC). The two labels are illustrated for 8-ASK in Table I.

C. PAS Transmitter

The PAS architecture implements probabilistically shaped ASK modulation. The PAS transmitter is displayed in Fig. 3 and works as follows (for a more detailed description, see [4, Sec. IV.]). A DM maps k data bits to n amplitudes A^n , which are represented by $n(m-1)$ amplitude bits. The amplitude bits and γn additional data bits are multiplied with the parity generating part \mathbf{P} of a systematic generator matrix $[\mathbf{I}|\mathbf{P}]$ to generate $(1-\gamma)n$ redundancy bits. The redundancy bits and the additional data bits are mapped to n signs S^n , which are multiplied symbolwise with the amplitudes A^n . The FEC code instantiated by \mathbf{P} has rate

$$c = \frac{n(m-1) + \gamma n}{mn} = \frac{m-1 + \gamma}{m} \quad (8)$$

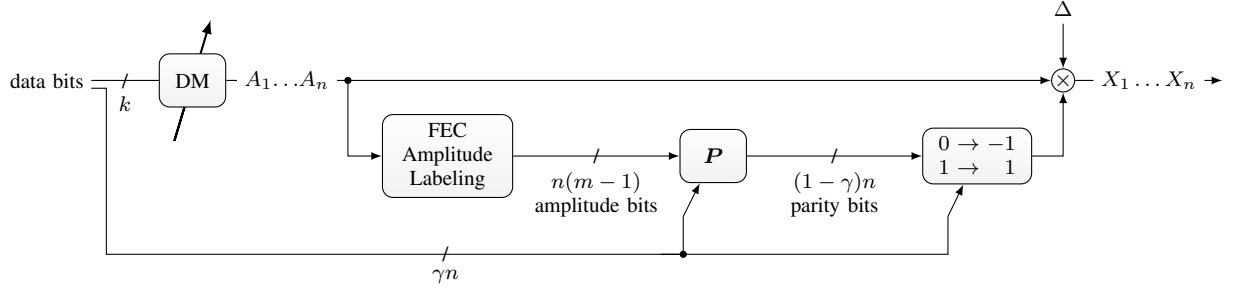


Fig. 3. The architecture of the PAS scheme. See Fig. 1 for a system view and [4, Sec. IV.] for a detailed description.

and the fraction of signs used for data bits is

$$\gamma = 1 - (1 - c)m. \quad (9)$$

PAS requires $0 \leq \gamma \leq 1$. The transmission rate of PAS is the number of data bits per ASK symbol given by

$$R_t = \frac{k}{n} + \gamma. \quad (10)$$

D. Channel Model

The generated signal points $A_i \cdot S_i$ are multiplied by the constellation scaling Δ and transmitted over an additive white Gaussian noise (AWGN) channel. We define $X_i = \Delta \cdot A_i \cdot S_i$. At a generic time instance, the channel model is

$$Y = X + Z \quad (11)$$

where Z is zero mean Gaussian noise with unit variance. The signal-to-noise ratio (SNR) is

$$\text{SNR} = \mathbb{E}[X^2]. \quad (12)$$

E. PAS Achievable Rate

We consider a PAS receiver with a bit-metric decoder. The PAS transmitter defines the label $\mathbf{B}^{\text{fec}} = \beta^{\text{fec}}(X)$ where $B_1^{\text{fec}} = B_1$ is the sign label and where $B_2^{\text{fec}} \dots B_m^{\text{fec}}$ is the amplitude label. We assume a uniform sign distribution, i.e.,

$$P_{B_1}(0) = P_{B_1}(1) = P_S(-1) = P_S(1) = \frac{1}{2}. \quad (13)$$

We refer to [4, Sec. IV.A] for a justification of this assumption. A binary demapper calculates the soft-informations

$$L_j = \log \frac{P_{B_j^{\text{fec}}}(0)}{P_{B_j^{\text{fec}}}(1)} + \log \frac{p_{Y|B_j^{\text{fec}}}(y|0)}{p_{Y|B_j^{\text{fec}}}(y|1)}, \quad j = 1, 2, \dots, m \quad (14)$$

which are passed to a binary decoder. By [19], an achievable rate for a bit-metric decoder is

$$R_{\text{bmd}} = \left[\mathbb{H}(X) - \sum_{j=1}^m \mathbb{H}(B_j^{\text{fec}}|Y) \right]^+ \quad (15)$$

where $[\cdot]^+ = \max(0, \cdot)$. For PAS, R_{bmd} must be evaluated using $P_X = P_A P_S$. The rate R_{bmd} is an achievable rate for the PAS receiver with BMD if

$$\mathbb{H}(A) + \gamma = R_{\text{bmd}}. \quad (16)$$

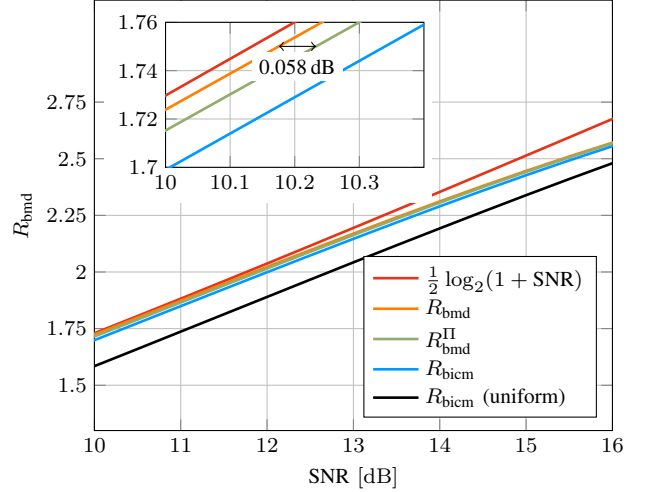


Fig. 4. Achievable rates for 8-ASK.

We will also need the relations between R_{bmd} , P_X , and SNR, namely

$$R = R_{\text{bmd}}(P_X, \text{SNR}) \quad (17)$$

$$\text{SNR} = R_{\text{bmd}}^{-1}(P_X, R). \quad (18)$$

III. PRODUCT DISTRIBUTION MATCHING

A. NBC Product Distributions

Suppose for some amplitude label $B_2^{\text{dm}} \dots B_m^{\text{dm}}$ and the corresponding signal point label $\mathbf{B}^{\text{dm}} = B_1 B_2^{\text{dm}} \dots B_m^{\text{dm}}$ we have

$$P_{\mathbf{B}^{\text{dm}}} = \prod_{j=1}^m P_{B_j^{\text{dm}}} \quad (19)$$

where $P_{B_1^{\text{dm}}} = P_{B_1}$. In particular, the amplitude distribution P_A is such that the bits of the label \mathbf{B}^{dm} are statistically independent. We can construct a distribution (19) by choosing an amplitude label and binary distributions $P_{B_j^{\text{dm}}}$, $j = 2, \dots, m$. Note that the generated distribution depends both on the label function and the binary distributions. An achievable rate is

$$R_{\text{bmd}}^{\text{II}} = \left[\sum_{j=1}^m \mathbb{H}(B_j^{\text{dm}}) - \sum_{j=1}^m \mathbb{H}(B_j^{\text{fec}}|Y) \right]^+. \quad (20)$$

Note that the label \mathbf{B}^{dm} is not required to be the same as the label \mathbf{B}^{fec} that is used by the FEC encoder and decoder. We choose the NBC for the amplitude label $B_2^{\text{dm}}, \dots, B_m^{\text{dm}}$, the BRGC for the FEC label \mathbf{B}^{fec} and we optimize (20) over the binary distributions $P_{B_j^{\text{dm}}}$, $j = 2, \dots, m$ (recall that the sign distribution P_{B_1} is uniform) and the constellation scaling Δ . In Fig. 4, we display the resulting achievable rate for 8-ASK. We observe that the product constraint (19) leads to virtually no performance loss.

Remark 1. *The information-theoretic work [20] considered only the case when $\mathbf{B}^{\text{dm}} = \mathbf{B}^{\text{fec}}$, in which case (20) becomes*

$$R_{\text{bicm}} = \sum_{j=1}^m \mathbb{I}(B_j^{\text{fec}}; Y) \quad (21)$$

which is the so-called BICM capacity. As shown in Fig. 4, R_{bicm} is less power efficient than $R_{\text{bmd}}^{\text{II}}$, although the difference is small.

B. PDM

PDM can efficiently generate the product distributions introduced in the previous subsection. The PDM is displayed in Fig. 2. k binary data bits are demultiplexed into $m - 1$ parallel blocks of lengths k_2 to k_m . The $m - 1$ parallel binary DMs output $m - 1$ shaped binary sequences of length n . A bit mapper χ_A^{dm} recombines the $m - 1$ sequences and outputs one shaped amplitude sequence of length n .

C. PDM Rate Loss

The rate and the output distribution of the j th DM is k_j/n and $P_{B_j^{\text{dm}}}$, respectively. The total rate of the PDM is

$$\frac{k}{n} = \frac{k_2 + \dots + k_m}{n} \quad (22)$$

and the total rate loss of the PDM is the sum of the individual rate losses, i.e.,

$$R_{\text{loss}} = \sum_{j=2}^m \left[\mathbb{H}(B_j^{\text{dm}}) - \frac{k_j}{n} \right]. \quad (23)$$

D. PDM for the AWGN Channel

For the AWGN channel, we use the NBC for the bit-mapper χ_A^{dm} and we choose binary DM distributions that minimize the overall power. Ignoring the rate loss for now, the optimization problem is

$$\begin{aligned} & \underset{P_{B_2}, \dots, P_{B_m}}{\text{minimize}} && \mathbb{E}[X^2] \\ & \text{subject to} && \sum_{j=2}^m \mathbb{H}(B_j) = R_{\text{dm}} \\ & && X = \chi^{\text{nbbc}}(\mathbf{B}). \end{aligned} \quad (24)$$

To account for the rate loss, we replace the sum-entropy constraint in (24) by a sum-rate constraint, where the j th rate k_j/n is the rate required to implement the DM output

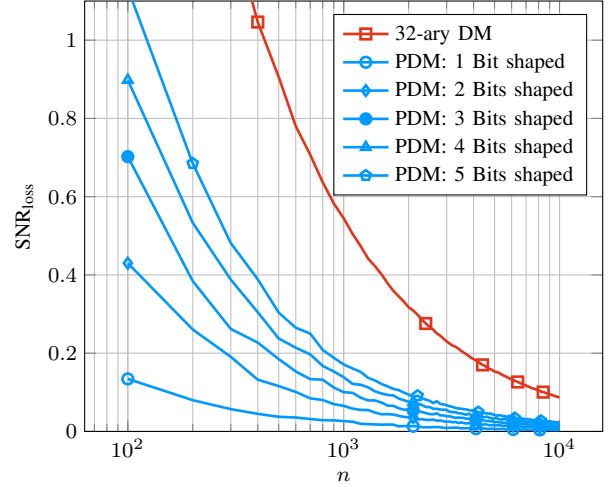


Fig. 5. Rate loss comparison for 64-ASK and SE = 4.5 bpcu.

distribution P_{B_j} . Altogether, we choose the component DMs via

$$\begin{aligned} & \underset{P_{B_2}, \dots, P_{B_m}}{\text{minimize}} && \mathbb{E}[X^2] \\ & \text{subject to} && \sum_{j=2}^m \frac{k_j}{n} = R_{\text{dm}} \\ & && X = \chi^{\text{nbbc}}(\mathbf{B}). \end{aligned} \quad (25)$$

E. Simulation Results

We numerically compare different DM implementations by using 64-ASK and a target SE of $R_t = 4.5$ bpcu. We employ a 32-ary DM as a reference as suggested in [4, Sec. V]. The performance of this system is compared to a PDM setup with 1 (B_2^{dm}), 2 ($B_2^{\text{dm}}, B_3^{\text{dm}}$), 3 ($B_2^{\text{dm}}, B_3^{\text{dm}}, B_4^{\text{dm}}$), 4 ($B_2^{\text{dm}}, B_3^{\text{dm}}, B_4^{\text{dm}}, B_5^{\text{dm}}$) and 5 ($B_2^{\text{dm}}, B_3^{\text{dm}}, B_4^{\text{dm}}, B_5^{\text{dm}}, B_6^{\text{dm}}$) individually shaped bit-levels and corresponding binary DMs. The product distribution has been obtained by following the approach of Sec. III-D, while imposing a uniform distribution on the unshaped bit-levels.

We first consider the results of Fig. 5 which illustrates the finite length loss of all considered configurations. The DM rate loss (4) and the PDM rate loss (23) is converted to an ‘‘SNR loss’’ by

$$\text{SNR}_{\text{loss}} = 10 \log_{10} \left(\frac{R_{\text{bmd}}^{-1}(P_X, R_t + R_{\text{loss}})}{R_{\text{bmd}}^{-1}(P_X, R_t)} \right). \quad (26)$$

As a rule of thumb, the following expression may be useful as a rough estimate:

$$\begin{aligned} \text{SNR}_{\text{loss,awgn}} &= 10 \log_{10} \left(\frac{2^{2(R_t + R_{\text{loss}})} - 1}{2^{2R_t} - 1} \right) \\ &\approx R_{\text{loss}} \cdot 20 \log_{10} 2 \approx R_{\text{loss}} \cdot 6 \text{ dB}. \end{aligned} \quad (27)$$

We observe that the PDMs have an aggregated rate loss that is significantly lower than the rate loss of the 32-ary DM. The resulting performance is comparable only for output lengths of more than 10^4 symbols.

To further illustrate the flexibility of the transmitter design, we consider a coded scenario with a rate 9/10 LDPC block

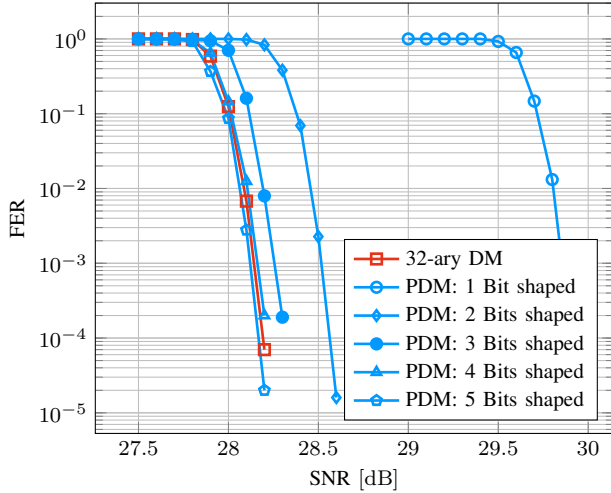


Fig. 6. Performance comparison of the proposed PDM for 64-ASK and a target SE of 4.5 bpcu and different number of shaped bits.

TABLE II
REQUIRED SNRS FOR DIFFERENT DM CONFIGURATIONS AND A TARGET SE OF 4.5 BPCU. (CAPACITY: 27.08 DB)

DM configuration	Required SNR [dB]
32-ary DM	27.13
PDM 1 Bit shaped	28.29
PDM 2 Bits shaped	27.48
PDM 3 Bits shaped	27.35
PDM 4 Bits shaped	27.32
PDM 5 Bits shaped	27.31

code from the DVB-S2 standard [21] of block length 64 800 bits and a corresponding DM output length of 10 800 symbols. This choice allows for a fair comparison, as both the parallel binary DMs and the 32-ary DM have a similar performance. Fifty iterations are used for the belief propagation (BP) decoding.

As shown in Fig. 6, a PDM with 3 shaped bit-levels achieves a similar performance as the 32-ary DM. If only 2 bit-levels are shaped, the loss in energy efficiency is 0.4 dB at a target frame error rate (FER) of 10^{-3} . Table II illustrates that these observations are reflected by the asymptotic achievable rates of Sec. II-E, which were evaluated for the corresponding optimized distributions. While the required SNRs to achieve an SE of 4.5 bpcu are close for 3, 4 and 5 shaped bit-levels, larger gaps can be observed for 1 or 2 shaped bit-levels.

IV. PROBABILISTIC SHAPING FOR PARALLEL CHANNELS

A. System Model

We consider L parallel channels with the I/O relation

$$Y_\ell = h_\ell X_\ell + Z_\ell, \quad \ell = 1, 2, \dots, L. \quad (28)$$

The noise terms Z_ℓ are zero mean Gaussian with unit variance. The h_ℓ model the channel gains and we assume that both the receiver and transmitter have full channel state information, i.e., they both know the channel gains h_ℓ and the noise variance. We consider coding over n channel uses of each channel, which results in total in $L \cdot n$ channel uses. This

choice is for clarity of exposition; the scheme can easily be generalized.

B. Waterfilling [22, Sec. 5.4.6]

The transmitter has an average power budget P , i.e., the inputs are subject to the sum-power constraint

$$\frac{1}{L} \sum_{\ell=1}^L \mathbb{E}[X_\ell^2] \leq P. \quad (29)$$

The average SE

$$\frac{1}{L} \sum_{\ell=1}^L \frac{1}{2} \log_2(1 + h_\ell^2 P_\ell) \quad (30)$$

is achievable with the channel inputs X_ℓ being independent zero mean Gaussian with variance P_ℓ . The average SE is maximized by waterfilling, i.e.,

$$P_\ell^* = \left[\frac{1}{\lambda} - \frac{1}{h_\ell^2} \right]^+, \quad \lambda: \frac{1}{L} \sum_{\ell=1}^L P_\ell^* = P. \quad (31)$$

Suppose that P_ℓ^* is positive. The SE allocated to channel ℓ is then

$$C_\ell = \frac{1}{2} \log_2 \frac{h_\ell^2}{\lambda}. \quad (32)$$

Based on C_ℓ , we choose the constellation size 2^{m_ℓ} so that

$$m_\ell \approx C_\ell + 1 \quad (33)$$

to avoid reduced SE because of too small constellation sizes. Let $m = \max_\ell m_\ell$ denote the maximum constellation size.

C. PAS for Parallel Channels

PAS can easily be combined with parallel channels. This is illustrated in Fig. 7. A DM device transforms data bits into a sequence of amplitudes for each channel, which are then combined with sign bits originating from a common encoding device. In its simplest form, this DM device consists of individual DMs, each with its output alphabet size matched to the corresponding constellation size, see Fig. 8.

D. PDM for Parallel Channels

The PDM suggests an alternative way to generate L amplitude sequences for distinct constellation sizes. For example, suppose we have $L = 2$ different channels and need a length n amplitude sequence for 4-ASK and a length n sequence for 8-ASK. The PDM needs one binary DM for 4-ASK and two binary DMs for 8-ASK. As illustrated in Fig. 10, the idea is now to use for the first amplitude bit-level B_2 of 4-ASK and 8-ASK a single binary DM with output length $n_2 = 2 \cdot n$ and to generate the second amplitude bit-level B_3 for 8-ASK by a second binary DM with output length $n_3 = n$. The potential benefit of this approach is twofold: first, using PDM should reduce the rate loss, and second, replacing two DMs of lengths n by one single DM of length $2 \cdot n$ should reduce the rate loss even further. Fig. 9 shows this extended PDM scheme. It provides the same interface to PAS as the naive approach that uses L individual DMs.

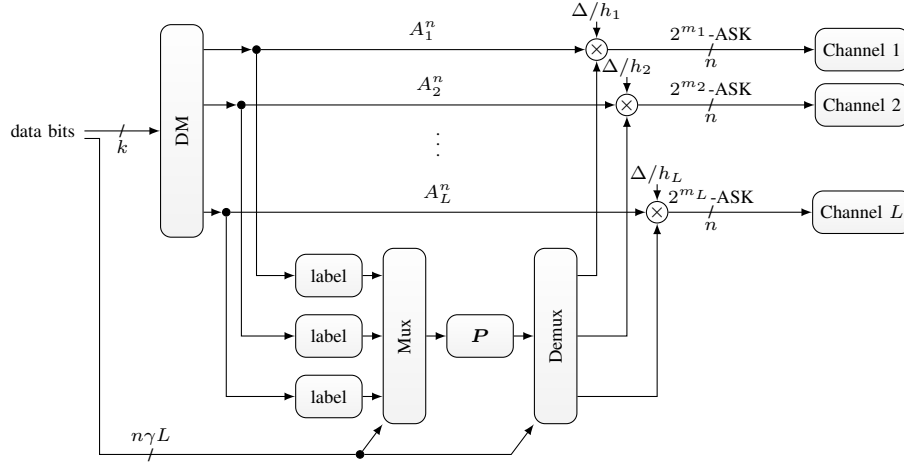


Fig. 7. Illustration of PAS for parallel channels. Each of the L channels has an individual constellation size 2^{m_ℓ} , $\ell = 1, 2, \dots, L$. PAS for parallel channels extends the PAS for single channels shown in Fig. 3. The constellation scalings Δ/h_ℓ are explained in Sec. IV-F. The DM device can be implemented by L individual DMs, as illustrated in Fig. 8, or by extended PDM illustrated in Fig. 9. Extended PDM can be much more power efficient, see Fig. 11 for an example.

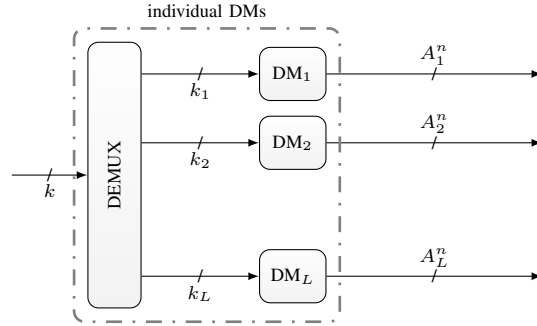


Fig. 8. Individual DM implementation for PAS for parallel channels shown in Fig. 7. The k data bits are demultiplexed and fed to L individual DMs.

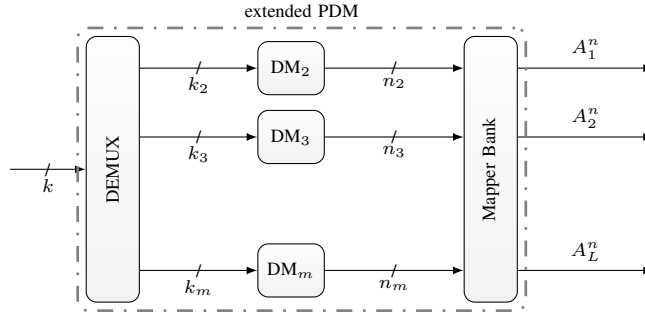


Fig. 9. Extended PDM implementing the DM of PAS for parallel channels shown in Fig. 7. The extended PDM transforms k data bits into L amplitude sequences of length n . Internally, the extended PDM uses $m - 1$ binary component DMs, where 2^m -ASK is the largest supported constellation. The output lengths n_2, \dots, n_m of the component DMs are given by (37). The input lengths fulfill $\sum_{j=2}^m k_j = k$ and reflect the component DM rates k_j/n_j .

Simultaneously using one DM on more than one constellation size imposes restrictions on the distribution families that can be generated by extended PDM. We next argue how extended PDM can be used to generate families of Gaussian-like distributions. The maximum constellation size is 2^m and we choose the $m - 1$ DM output distributions so that an NBBC mapper generates a Gaussian-like distribution. By grouping 2^j neighbouring signal points together, the distribution of these signal point groups is still Gaussian-like, and it is given by the product distribution generated by the first $m - 1 - j$ DMs. This suggests that by using only $m - 1$ DMs, we can simultaneously generate Gaussian-like distributions on

$4, 8, \dots, 2^m$ -ASK constellations. An example is shown in Fig. 10.

E. Parametrization

We next state the parameters of the FEC code and the PDM so that the parallel PAS operates at a specific SE. For the considered case where we use each of the L channels n times, the block length of the binary FEC code is

$$n_{\text{code}} = \sum_{\ell=1}^L m_\ell \cdot n \quad (34)$$

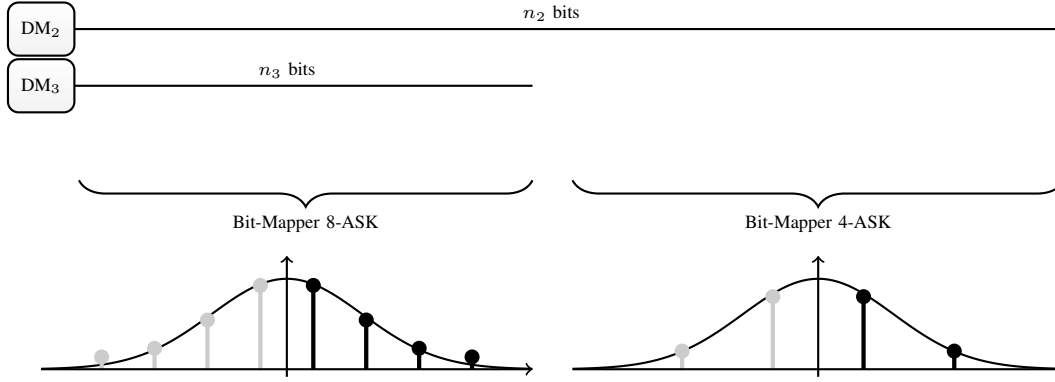


Fig. 10. Simultaneously generating two Gaussian-like amplitude distributions for 4-ASK and 8-ASK by reusing the DM of bit-level 2.

and formulas (8) and (9) generalize to

$$c = \frac{\sum_{\ell=1}^L (m_{\ell} - 1 + \gamma)}{\sum_{\ell=1}^L m_{\ell}} \quad (35)$$

$$\gamma = 1 - (1 - c) \frac{1}{L} \sum_{\ell=1}^L m_{\ell}. \quad (36)$$

The DM output lengths are given by

$$n_j = \sum_{\ell=1}^L \mathbf{1}(m_{\ell} \geq j) \cdot n, \quad j = 2, 3, \dots, m \quad (37)$$

and the corresponding DM input lengths are k_2, k_3, \dots, k_m . The average SE of the overall system is now

$$R_t = \frac{\sum_{j=2}^m k_j}{L \cdot n} + \gamma \quad (38)$$

$$= \frac{1}{L \cdot n} \left[\sum_{j=2}^m \mathbb{H}(B_j^{\text{dm}}) n_j \right] + \gamma - R_{\text{loss}}. \quad (39)$$

F. Waterfilling for PAS

For the L parallel channels, suppose we have chosen the constellation sizes $2^{m_{\ell}}$, $\ell = 1, \dots, L$ and suppose further we have chosen the code rate c and thereby the fraction γ of signs used for data bits. To achieve the target rate R_t , the rate assigned to the amplitudes is thus $R_{\text{dm}} = R_t - \gamma$, which results in the following constraint for the amplitude distributions (ignoring the rate loss):

$$\frac{1}{L} \sum_{\ell=1}^L \mathbb{H}(A_{\ell}) = R_{\text{dm}}. \quad (40)$$

Recall that the inputs X_{ℓ} are given by $\Delta_{\ell} A_{\ell} S_{\ell}$ where

$$A_{\ell} S_{\ell} \in \{\pm 1, \pm 3, \dots, \pm(2^{m_{\ell}} - 1)\}. \quad (41)$$

The average power on the ℓ th channel is $\mathbb{E}[(\Delta_{\ell} A_{\ell})^2]$ and depends on the distribution $P_{A_{\ell}}$ and the constellation scaling Δ_{ℓ} . We use the following strategy: to ensure a similar detection reliability on each channel, independent of the chosen amplitude distributions, we choose

$$\Delta_{\ell} = \frac{\Delta}{h_{\ell}}. \quad (42)$$

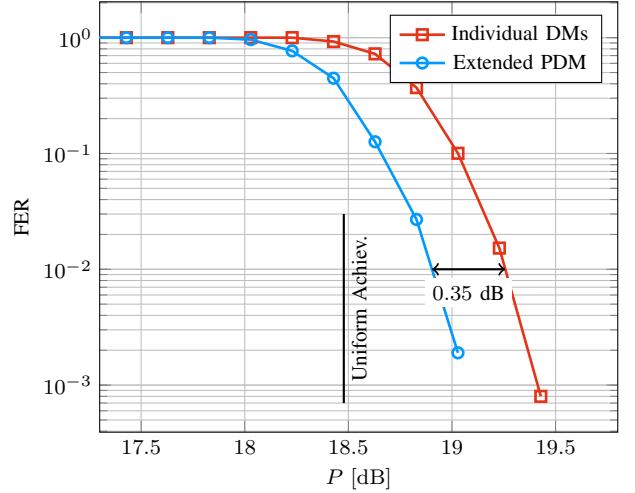


Fig. 11. Coded performance comparison of individual DMs and extended PDM (LDPC code with block length 5184 bits) for parallel channels.

In this way, two neighbouring constellation points have the distance 2Δ on all channels. The average power on each channel is $\frac{\Delta^2}{h_{\ell}^2} \mathbb{E}[A_{\ell}^2] \propto \frac{1}{h_{\ell}^2} \mathbb{E}[A_{\ell}^2]$. Next, we calculate the amplitude distributions by

$$\text{minimize}_{P_{A_1}, \dots, P_{A_L}} \sum_{\ell=1}^L \frac{1}{h_{\ell}^2} \mathbb{E}[A_{\ell}^2] \quad (43)$$

$$\text{subject to} \quad \frac{1}{L} \sum_{\ell=1}^L \mathbb{H}(A_{\ell}) = R_{\text{dm}}. \quad (44)$$

To account for rate loss, the sum-entropy constraint is replaced by a DM sum-rate constraint. For extended PDM, the sum-entropy and sum-rate expressions from (39) and (38) are used, respectively.

G. Simulation Results

To evaluate the performance of parallel PAS and extended PDM, we employ the following example of 3 parallel channels,

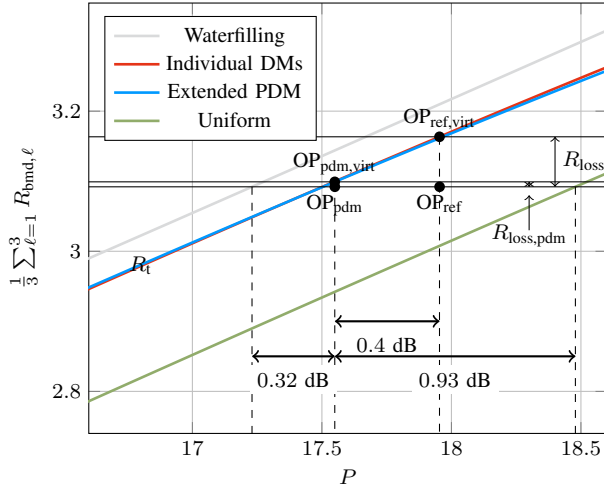


Fig. 12. Asymptotic analysis of the incurred rate loss.

TABLE III
PROPERTIES OF THE EXTENDED PDM SETUP

DM _j	n _j	P _{B_j^{dm}} (0)	H(B _{j^{dm}})
2	1296	0.2522	0.8148
3	1296	0.3940	0.9674
4	864	0.4474	0.9920
5	432	0.4674	0.9969

given as

$$\begin{aligned} Y_1 &= 2.0 \cdot X_1 + Z_1 \\ Y_2 &= 1.3 \cdot X_2 + Z_2 \\ Y_3 &= 0.6 \cdot X_3 + Z_3 \end{aligned}$$

and an average power constraint of $P = 17.23$ dB. Performing the waterfilling as shown in Sec. IV-B, we arrive at the following rate assignment:

$$\begin{aligned} C_1 &= 3.87 \\ C_2 &= 3.25 \\ C_3 &= 2.14. \end{aligned}$$

Consequently, we target an SE of $R_t = \frac{1}{3} \sum_{\ell=1}^3 C_\ell = 3.09$ bpcu and select constellation sizes of $2^{m_1} = 32$, $2^{m_2} = 16$ and $2^{m_3} = 8$ points following (33). We use each of the three channels $n = 432$ times.

As a reference, we choose an architecture with individual 16-ary, 8-ary and 4-ary DMs. For the PDM setup, we employ four parallel binary DMs. Their respective output lengths and distributions are summarized in Table III. We have a maximum constellation size of 32-ASK, i.e., four bits can be shaped. Bit-levels 2 and 3 are shared by all three constellations, whereas bit-level 4 is used only by 16-ASK and 32-ASK. Bit-level 5 appears in 32-ASK only. The distributions of the individual DMS and the binary distribution of the extended PDM have been chosen following Sec. IV-F.

In the following, we use a block length 5184 LDPC code of rate $c = 5/6$ from the G.hn standard [23]. As before, 50 BP iterations are performed.

Observe in Fig. 11 that the PDM setup improves over the reference strategy at a FER of 10^{-2} by 0.35 dB. This is mainly because of the decreased rate loss as shown in the asymptotic achievability plot of Fig. 12. We plot the average achievable rate over all parallel channels vs. the average sum power for both schemes and their specific input distributions. The power assignment is optimized via mercury/waterfilling. We also plot three horizontal lines at 3.09 bpcu, 3.099 bpcu and 3.16 bpcu, which denote R_t , $R_t + R_{\text{loss,pdm}}$ and $R_t + R_{\text{loss,ref}}$, respectively. The crossing of the last two horizontal lines with their respective achievability curves are labeled as $\text{OP}_{\text{pdm,virt}}$ and $\text{OP}_{\text{ref,virt}}$. They indicate virtual operating points that would be achievable with the currently used input distributions. Because of the rate loss, the actual operating points are given by the orthogonal projections of these points on the actual SE curve, however. Their difference in SNR of 0.4 dB accurately predicts the gap of 0.35 dB that we observe in the coded result in Fig. 11. Compared to uniform distributions, the asymptotic gain (accounting for the rate loss) is 0.93 dB. The gap to the waterfilling solution is 0.32 dB.

V. CONCLUSION

We proposed product distribution matching (PDM), an architecture that uses binary DMs in parallel. This parallelization enables high-throughput implementations of DMs. The binary component DMs of PDM reduce complexity. We have shown that PDM performs as well as higher-order DMs for long block lengths and that PDM can perform much better than higher-order DMs for short block lengths. We have proposed extended PDM, which enables PAS to operate close to the waterfilling limit of multi-carrier transmission schemes such as OFDM.

ACKNOWLEDGMENT

The authors would like to thank Gerhard Kramer for fruitful discussions and comments on drafts of this manuscript.

REFERENCES

- [1] *Digital Video Broadcasting (DVB); Second generation framing structure, channel coding and modulation systems for Broadcasting, Interactive Services, News Gathering and other broadband satellite applications; Part 2: DVB-S2 Extensions (DVB-S2X)*, European Telecommun. Standards Inst. (ETSI) Std. EN 302 307-2, Rev. 1.1.1, 2014.
- [2] M. F. Barsoum, C. Jones, and M. Fitz, "Constellation Design via Capacity Maximization," in *Proc. IEEE Int. Symp. Inf. Theory (ISIT)*, Jun. 2007, pp. 1821–1825.
- [3] N. S. Lohin, J. Zöllner, B. Mouhouche, D. Anzorregui, J. Kim, and S. I. Park, "Non-Uniform Constellations for ATSC 3.0," *IEEE Trans. Broadcast.*, vol. 62, no. 1, pp. 197–203, Mar. 2016.
- [4] G. Böcherer, F. Steiner, and P. Schulte, "Bandwidth efficient and rate-matched low-density parity-check coded modulation," *IEEE Trans. Commun.*, vol. 63, no. 12, pp. 4651–4665, 2015.
- [5] G. Böcherer and R. Mathar, "Matching dyadic distributions to channels," in *Proc. Data Compression Conf.*, Snowbird, UT, USA, 2011, pp. 23–32.
- [6] P. Schulte and G. Böcherer, "Constant composition distribution matching," *IEEE Trans. Inf. Theory*, vol. 62, no. 1, pp. 430–434, 2016.
- [7] P. Yuan, "Rate-matched coded modulation for wireless transmission," Master's thesis, Technical University of Munich, Institute for Communications Engineering, 2015.
- [8] F. Buchali, F. Steiner, G. Böcherer, L. Schmalen, P. Schulte, and W. Idler, "Rate adaptation and reach increase by probabilistically shaped 64-QAM: An experimental demonstration," *J. Lightw. Technol.*, vol. 34, no. 8, Apr. 2016.

- [9] T. Prinz, "Polar codes for higher-order modulation and probabilistic amplitude shaping," Master's thesis, Technical University of Munich, Institute for Communications Engineering, 2016.
- [10] J. J. Boutros, F. Jardel, and C. Méasson, "Probabilistic shaping and non-binary codes," *arXiv preprint arXiv:1701.07976*, 2017.
- [11] F. Steiner and G. Böcherer, "Comparison of Geometric and Probabilistic Shaping with Application to ATSC 3.0," in *Int. ITG Conf. Source Channel Coding*, Hamburg, Germany, Feb. 2017.
- [12] "Signal shaping for QAM constellations," Huawei, Athens, Greece, Tech. Rep., Feb. 2018, 3GPP TSG-RAN no. 88. [Online]. Available: http://www.3gpp.org/ftp/tsg_ran/WG1_RL1/TSGR1_88/Docs/R1-1701712.zip
- [13] W. Idler, F. Buchali, L. Schmalen, E. Lach, R.-P. Braun, G. Böcherer, P. Schulte, and F. Steiner, "Field trial of a 1 Tbit/s super-channel network using probabilistically shaped constellations," *J. Lightw. Technol.*, vol. 99, no. PP, pp. 1–1, 2017.
- [14] K. Roberts, Q. Zhuge, I. Monga, S. Gareau, and C. Laperle, "Beyond 100 Gb/s: Capacity, Flexibility, and Network Optimization," *Journal of Optical Communications and Networking*, vol. 9, no. 4, pp. C12–C24, Apr. 2017.
- [15] P. Schulte and B. C. Geiger, "Divergence scaling of fixed-length, binary-output, one-to-one distribution matching," *arXiv preprint arXiv:1701.07371*, 2017.
- [16] <http://www.shapecomm.de>.
- [17] T. Ramabadran, "A coding scheme for m-out-of-n codes," *IEEE Trans. Commun.*, vol. 38, no. 8, pp. 1156–1163, Aug. 1990.
- [18] F. Gray, "Pulse code communication," U. S. Patent 2 632 058, 1953.
- [19] G. Böcherer, "Achievable rates for shaped bit-metric decoding," *arXiv preprint*, 2014. [Online]. Available: <http://arxiv.org/abs/1410.8075>
- [20] A. G. i Fabregas and A. Martinez, "Bit-interleaved coded modulation with shaping," in *Proc. IEEE Inf. Theory Workshop (ITW)*, 2010.
- [21] *Digital Video Broadcasting (DVB); 2nd Generation Framing Structure, Channel Coding and Modulation Systems for Broadcasting, Interactive Services, News Gathering and Other Broadband Satellite Applications (DVB-S2)*, Std. EN 302 307, Rev. 1.2.1, 2009.
- [22] D. Tse and P. Viswanath, *Fundamentals of wireless communication*. Cambridge university press, 2005.
- [23] *Unified high-speed wire-line based home networking transceivers - System architecture and physical layer specification*, ITU Std. G.9960, Oct. 2010.